Inorganic Chemistry

Article

pubs.acs.org/IC

Enhancing the Anion Affinity of Urea-Based Receptors with a Ru(terpy)$_2^{2+}$ Chromophore

Giorgio Baggi,[†] Massimo Boiocchi,[‡] Carlo Ciarrocchi,[†] and Luigi Fabbrizzi*[,†]

[†]Dipartimento di Chimica and [‡]Centro Grandi Strumenti, Università di Pavia, 27100 Pavia, Italy

Supporting Information

ABSTRACT: Covalent linking of a Ru(terpy)$_2^{2+}$ substituent improves recognition and sensing properties of the urea subunit toward anions. Urea's anion affinity is enhanced by the electrostatic attraction exerted by the Ru^{II} cation and by the electron-withdrawing effect exerted by the entire polypyridine–metal complex. Such an enhancement of the anion affinity, which results from the combination of a through-space and a through-bond effect, is greater than that exerted by the classical neutral electron-withdrawing substituent nitrophenyl. Small yet significant modifications of $\pi-\pi^*$ and MLCT bands of the Ru(terpy)$_2^{2+}$ chromophore, detected through UV–vis spectrophotometric titrations, allowed the determination of the constants for the formation of receptor–anion H-bond complexes in diluted MeCN solution. On ^{1}H NMR titration experiments, carried out under more concentrated conditions, the interaction of a second Cl$^-$ ion was observed, taking place through an outer-sphere mechanism. The Ru(terpy)$_2^{2+}$ substituent favors the deprotonation of a urea N–H fragment on addition of a second equivalent of fluoride, with formation of HF_2^-.

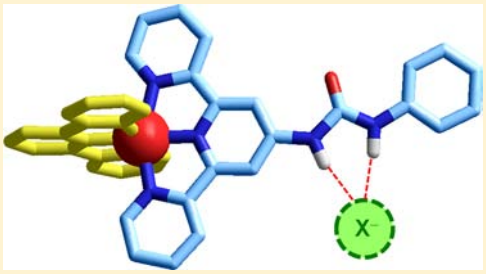

INTRODUCTION

The affinity toward inorganic anions of organic receptors behaving as H-bond donors is typically assessed through titration experiments in aprotic media ($CHCl_3$, CH_3CN, or DMSO, in order of increasing polarity).[1] Observed quantities are in general the chemical shifts, δ, of selected protons (^{1}H NMR titrations) and the energy and the intensity of absorption bands in the UV–vis region (spectrophotometric titrations). The ^{1}H NMR titration in deuterated solvents is convenient in different aspects, because it provides also useful pieces of information on the atoms directly involved in the anion binding and on the structural rearrangements, if any, accompanying the complexation process. An intrinsic disadvantage associated with this method is related to the relatively high concentrations required for the ^{1}H NMR experiment ($\geq 10^{-3}$ M), which prevents a safe determination of binding constants $K > 10^4$. In spectrophotometric titrations, the receptor must be equipped with a covalently linked chromophore the spectral features of which should be modified as a consequence of anion interaction. As an example, the classical chromophore nitrophenyl ($\varepsilon \approx 20\,000$ M^{-1} cm^{-1} at $\lambda_{max} = 380$ nm), which can be covalently linked to a receptor's backbone through simple synthetic procedures, ensures the observation of significant spectral modifications for concentrations as low as 10^{-6} M. This allows the determination of binding constants as high as 10^7 (being very careful in avoiding the interference of impurities, including water).

In this work, we consider as a reporter of receptor–anion interaction an inorganic chromophore, Ru^{II}(terpy)$_2^{2+}$ (terpy = 2,2′:6′,2″-terpyridine), which shows a rather intense metal-to-ligand charge transfer (MLCT) band in the visible region ($\varepsilon \approx$ 20 000 M^{-1} cm^{-1} at $\lambda_{max} = 480$ nm). In particular, we considered the derivative $[L^1H]^{2+}$ in which a Ru^{II}(terpy)$_2^{2+}$ subunit has been linked to a phenylurea moiety.

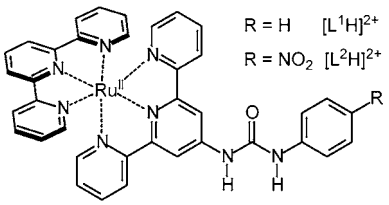

Urea is a classical neutral receptor capable of recognizing anions by hydrogen bonding whose interaction with anions has been extensively investigated through ^{1}H NMR spectroscopy, spectrophotometry, spectrofluorimetry, and voltammetry.[2] Urea can interact with a single acceptor atom (e.g., that of a halide ion), thus forming a six-membered chelate ring, or with two adjacent oxygen atoms of an oxoanion to give an eight-membered chelate ring. Since the appearance of the seminal papers by Wilcox[3] and Hamilton,[4] a variety of receptors containing one or more urea moieties have been synthesized over the last 2 decades. In particular, attention has been devoted to *N*,*N*′-substituted ureas, with the aim of controlling through the choice of the substituents the polarization of the N–H fragments and, ultimately, the receptor's binding tendencies toward anions.

In this perspective, we consider here also the urea derivative $[L^2H]^{2+}$, containing a nitrophenyl group as an additional substituent. The nitrophenyl group is both a sensitive

Received: January 25, 2013
Published: April 11, 2013

   dx.doi.org/10.1021/ic400196a | *Inorg. Chem.* 2013, 52, 5273–5283

chromophore and a powerful electron-withdrawing substituent capable of highly polarizing the adjacent urea N−H fragment, a feature that, in the presence of the F^- ion, may lead to N−H deprotonation and formation of the HF_2^- ion.[5] This study is aimed (i) to evaluate the capability of the $Ru^{II}(terpy)_2^{2+}$ subunit to act as an optical reporter (absorbance) and (ii) to assess its ability to polarize the N−H fragment and control the H-bond tendencies toward anions. Combined ^1H NMR and spectrophotometric titration experiments helped to sketch a clear picture of the interaction of $[L^1H]^{2+}$ and $[L^2H]^{2+}$ with anions and to throw further light on the intriguing topic of the solution behavior of N−H-containing receptors.[6]

The most classical of luminescent metal complexes, $Ru^{II}(bpy)_3^{2+}$ (bpy = 2,2′-bipyridine), has been covalently linked to a variety of receptors containing amide N−H fragments as H-bond donors and has been extensively investigated as an optical reporter for anion sensing.[7−11] Interaction with anions induced in most cases a moderate bathochromic shift and a substantial increase of the intensity of the emission band, which was ascribed to an increased rigidity of the molecular system and to the consequent decreased possibility of a vibrational deactivation. However, chirality makes complexes of the $Ru(bpy)_3^{2+}$ family unsuitable for the construction of metallosupramolecular systems. On the other hand, $Ru^{II}(terpy)_2^{2+}$ is achiral and allows easy functionalization at position 6 of the terpy molecule, which opens the way to the synthesis of symmetrical derivatives and favors a thorough investigation of substituent effects.[12] However, $Ru^{II}(terpy)_2^{2+}$ cannot compete with $Ru^{II}(bpy)_3^{2+}$ as a luminophore for sensing, because it is not luminescent in solution at room temperature, displaying a definite emission spectrum only at low temperature (e.g., in a matrix at 77 K).[13] Nevertheless, insertion in position 6 of the terpy ligand of an electron-withdrawing/electron-donor substituent may induce an increase of the lifetime of the ^3MLCT excited state and an increase of the emission intensity.[14] Thus, appropriate substitution at position 6 has produced some luminescent homo- and heteroleptic $Ru^{II}(terpy)_2^{2+}$ derivatives suitable for anion sensing. In particular, the heteroleptic complex $Ru^{II}(terpy)(terpy\text{-}L)^{2+}$, in which a $Cu^{II}(cyclam)^{2+}$ moiety has be covalently linked at position 6 of a terpy group,[15] is not luminescent in aqueous MeCN at room temperature, due to the occurrence of an electron transfer process from the Cu^{II} center to the photoexcited luminophore, which quenches emission. Added anions (halides, hydroxide) stabilize the $Cu^{II}(cyclam)^{2+}$ complex through apical coordination, which alters the Cu^{II}/Cu^{I} redox potential and prevents the electron transfer process. Thus, anion recognition is signaled by a sharp revival of luminescence.[16] More recently, one terpy moiety of $Ru^{II}(terpy)_2^{2+}$ has been functionalized with a side chain containing an imidazole ring, whose N−H fragment acts as the binding site for anions.[17] The complex is luminescent and is quenched on interaction with F^-.

RESULTS AND DISCUSSION

The X-ray Structure of the $[L^1H](PF_6)_2\cdot1.75H_2O$ Complex Salt. Crystals of $[L^1H](PF_6)_2\cdot1.75H_2O$ were obtained by diffusion of diethyl ether on an MeCN solution of the complex salt, whose structure is shown in Figure 1.

The two 2,2′:6′,2″-terpyridine moieties behave as terdentate ligands and the Ru^{II} metal center exhibits a distorted octahedral geometry, with the two ligands arranged according to a meridional coordination. Deviations for the N−Ru−N bond angles from the ideal value of 90° are most pronounced for the angles involving the N atom of a terminal ring (N in 2-position, N^2) and the N atom of a central ring (N in 6-position, N^6); the observed N^2−Ru−N^6 angles fall in the range 78.0(8)−102.7(6)°. The mean Ru−N^2 distances (2.038(14) Å for the nonsubstituted terpyridine moiety and 2.081(17) Å for the other one) are longer than the two Ru−N^6 distances (1.996(13) Å for the nonsubstituted terpyridine moiety and 2.007(14) Å for the other one). All these features can be ascribed to the rigidity of the terdentate ligand and are commonly observed in similar ruthenium(II) complexes in the literature. For instance, inspection of structures of bis-(2,2′:6′,2″-terpyridine)−ruthenium(II) complexes occurring in the CSD database system (2012 release)[18] shows that the Ru−N^2 distances are in the range 2.05−2.10 Å, whereas the Ru−N^6 distances fall in the range 1.97−2.02 Å.

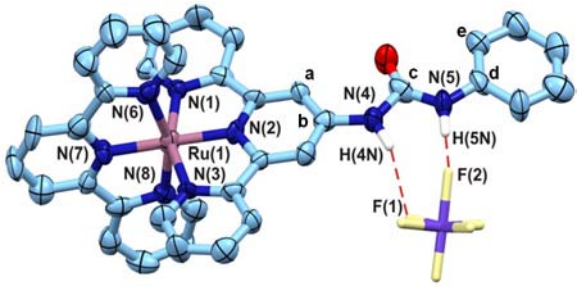

Figure 1. The crystal and molecular structure of the $[L^1H](PF_6)_2\cdot1.75H_2O$ complex salt (ellipsoids are drawn at the 30% probability level; one PF_6^- counterion and disordered water molecules have been omitted for clarity; atom names are reported only for atom sites bonded to the metal center and for atoms involved in H-bonds; only H atoms of the urea N−H fragments are shown). Selected features of the distorted octahedral Ru^{II} coordination are Ru(1)−N(1) 2.04(1), Ru(1)−N(2) 2.00(1), Ru(1)−N(3) 2.04(1), Ru(1)−N(6) 2.09(2), Ru(1)−N(7) 2.01(1), Ru(1)−N(8) 2.07(2) Å; N(1)−Ru(1)−N(2) 78.2(6)°, N(1)−Ru(1)−N(6) 90.0(6)°, N(1)−Ru(1)−N(7) 102.7(6)°, N(1)−Ru(1)−N(8) 93.1(5)°, N(2)−Ru(1)−N(3) 79.8(6)°, N(2)−Ru(1)−N(6) 102.1(7)°, N(2)−Ru(1)−N(8) 100.2(7)°, N(3)−Ru(1)−N(6) 94.5(6)°, N(3)−Ru(1)−N(7) 99.4(6)°, N(3)−Ru(1)−N(8) 91.0(6)°, N(6)−Ru(1)−N(7) 78.0(8)°, N(7)−Ru(1)−N(8) 79.6(7)°.

The two terpy moieties are essentially planar, the dihedral angles between the central and terminal pyridine rings of each terpyridine moiety lying in the range 2.6(12)−5.1(11)°. Moreover, the two terpy subunits are nearly orthogonal: in fact, the dihedral angle between the best planes of two coordinating terpyridine moieties is 88.7(2)°. The Ru^{II} metal center lies almost in these best planes, being displaced by 0.04(1) Å with respect to the best plane of the nonsubstituted terpy moiety and by 0.08(1) Å with respect to the other one. The entire terpy substituted molecule, coordinated to Ru^{II}, is flat and roughly planar. In fact, the dihedral angle between the best plane of the terpy moiety and the urea subunit is 11.2(13)°; the dihedral angle between the urea subunit and the terminal phenyl ring is 5.7(17)°; the dihedral angle between the terpyridine moiety and the phenyl ring is 16.8(11)°. On the other hand, the dihedral angle a−b−N_4−c (terpy-urea) is 2(3)°, while the dihedral angle c−N_5−d−e (urea-phenyl) is 5(3)°. On these structural bases, an extended π-delocalization over the entire molecular framework can be anticipated.

It is finally observed that one of the two PF_6^- counterions is definitely involved in a H-bond interaction with the urea subunit. In particular, each of the two contiguous fluorine

dx.doi.org/10.1021/ic400196a | Inorg. Chem. 2013, 52, 5273−5283

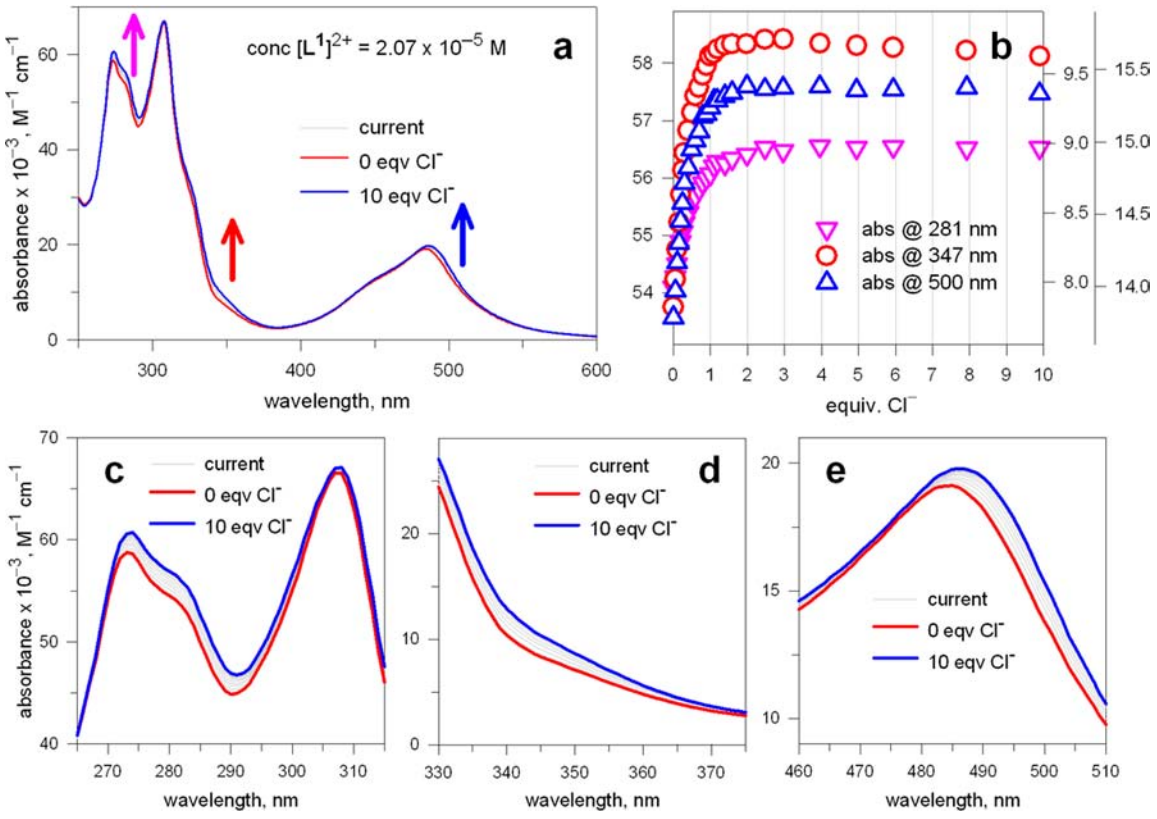

Figure 2. (a) Family of spectra taken over the course of the titration of a 2.07×10^{-5} M solution of $[[L^1H](PF_6)_2$ with a standard solution of $[Bu_4N]Cl$; (b) titration profiles at selected wavelengths; (c, d) details of the spectral modifications observed over the course of the titration in the $\pi-\pi^*$ region; (e) MLCT region.

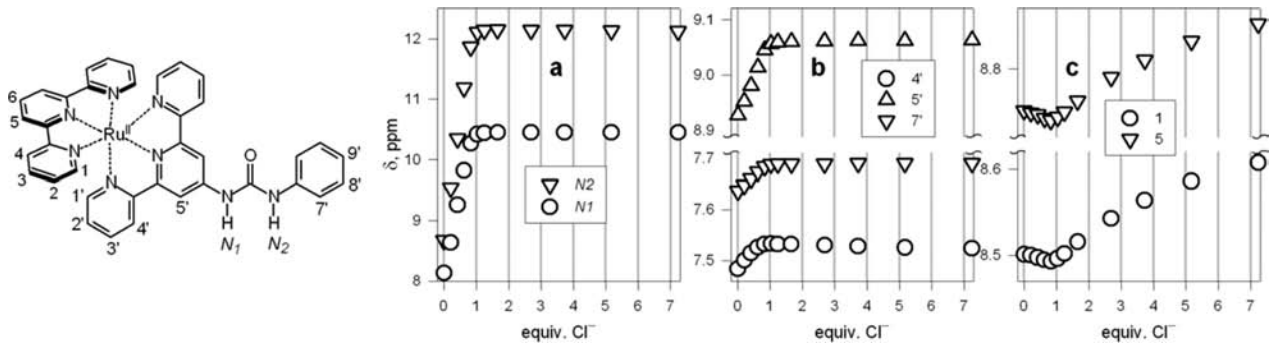

Figure 3. ^1H NMR titration profiles, based on the chemical shifts δ, for a CD_3CN solution of 3.5×10^{-3} M $[L^1H](PF_6)_2$, titrated with a standard solution of $[Bu_4N]Cl$.

atoms of PF_6^- interacts with one N−H fragment (see Figure 1). Features of these H-bond interactions are N(4)···F(1) 3.08(2) Å, H(4N)···F(1) 2.19(14) Å, N(4)−H(4N)···F(1) 152(11)°; N(5)···F(2) 3.03(3) Å, H(5N)···F(2) 2.14(13) Å, and N(5)−H(5N)···F(2) 155(11)°. The plane of the urea subunit and that containing the F−P−F atoms involved in the interaction form an angle of 63.4(10)°.

The Interaction of $[L^1H]^{2+}$ with Anions in Solution. The $[L^1H]^{2+}$ receptor was isolated as an hexafluorophosphate salt because PF_6^- is a rather poor H-bond acceptor and, in equimolar concentration, does not compete in solution with most anions (e.g., halides) for the receptor. Moreover, in titration experiments in MeCN, anions were added as $[Bu_4N]^+$ salts, in order to minimize the cation−anion electrostatic interaction and the formation of ion pairs. The interaction of $[L^1H]^{2+}$ and $[L^2H]^{2+}$ with HSO_4^- and $H_2PO_4^-$ could not be investigated due to formation of a precipitate.

$[L^1H]^{2+}$ in MeCN shows an absorption spectrum substantially similar to that of the model complex $[Ru^{II}(terpy)_2]^{2+}$ in the same medium. In particular only a moderate bathochromic shift of the MLCT band is observed (see Figure S1, Supporting Information). Figure 2 shows the family of spectra recorded over the course of the titration of a solution of 2.07×10^{-5} M $[L^1H](PF_6)_2$ with a standard solution of $[Bu_4N]Cl$. Small yet significant spectral changes have been observed both in the $\pi-\pi^*$ region (see Figure 2c,d) and in the MLCT region (Figure 2e). Titration profiles at selected wavelengths show saturation on addition of 1 equiv of chloride (see Figure 2b). The formation of a receptor−anion complex of 1:1 stoichiometry was confirmed by a Job plot at 500 nm (see Figure S2a, Supporting Information). On fitting of titration

dx.doi.org/10.1021/ic400196a | Inorg. Chem. 2013, 52, 5273−5283

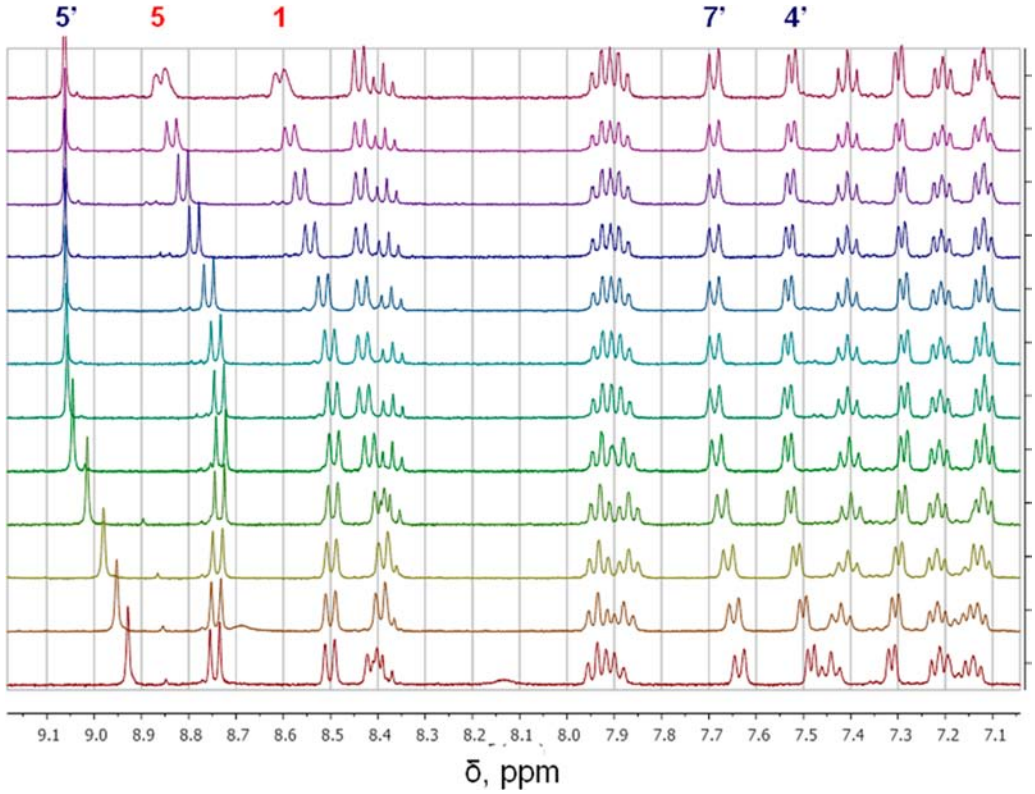

Figure 4. ^{1}H NMR spectra taken over the course of the titration with $[Bu_4N]Cl$ of a CD_3CN solution of 3.49×10^{-3} M $[L^1H](PF_6)_2$. Equivalent of Cl^- added (from the bottom): 0.00, 0.21, 0.41, 0.62, 0.83, 1.03, 1.24, 1.66, 2.69, 3.72, 5.17, and 7.24.

data through a nonlinear least-squares procedure,[19] over the 250−600 nm interval, log K = 5.66 ± 0.01 was calculated for the equilibrium:

$$[L^1H]^{2+} + Cl^- \leftrightarrows [L^1H\cdots Cl]^+ \quad (1)$$

More detailed pieces of information on the interaction of $[L^1H]^{2+}$ with Cl^- were obtained from a ^{1}H NMR titration experiment. In particular, a CD_3CN solution of 3.49×10^{-3} M $[L^1H](PF_6)_2$ (i.e., 175-fold more concentrated than that investigated in the UV−vis studies) was titrated with a standard solution of $[Bu_4N]Cl$. N−H protons of the urea subunits were observed at ∼8.75 ppm (N_1) and at 8.13 ppm (N_2) (see Figure S8 in the Supporting Information). On chloride addition, both signals experienced a drastic downfield shift, ascribed to an electrostatic effect. The greater shift felt by the N_1 proton with respect to N_2 indicates establishment of a more intense H-bond interaction with Cl^-, ascribed to the polarizing effect exerted by the $Ru(terpy)_2^{2+}$ substituent on the nearby N−H fragment.

Figure 3a shows the titration profiles based on the chemical shifts δ of N_1 and N_2 protons: the two profiles reach a plateau on addition of 1 equiv of anion, which confirms the occurrence of equilibrium 1. The absence of a smooth curvature in both profiles prevented a safe evaluation of the association constant.

Figure 4 shows the family of spectra (C−H portion) taken over the course of the titration. Protons 4′, 5′ (belonging to the terpy subunit linked to the urea moiety), and 7′ (belonging to the phenyl substituent of urea) undergo a significant downfield shift over the 0−1 equiv addition of chloride, then reach a definite plateau (see profiles in Figure 3b). Such a behavior is consistent with Cl^- binding to urea and with the establishment of an electrostatic interaction between the anion and the nearby protons. It is worth noting that the downfield shift experienced by proton 5′ is distinctly larger than that experienced by proton 7′, symmetrically positioned on the other side of the urea subunit. This strengthens the hypothesis of the higher acidity of the N−H fragment close to the Ru^{II} center.

The behavior of protons 1 and 5, belonging to the plain terpy molecule, is peculiar: they undergo a moderate upfield shift on 0−1 equiv addition of chloride but experience a pronounced downfield shift on further addition of Cl^- (see profiles in Figure 2c).

It is suggested that such an effect is exerted by a second Cl^- ion electrostatically interacting with the $Ru(terpy)_2^{2+}$ moiety in a definite outer-sphere complex, which forms according to equilibrium 2:

$$[L^1H\cdots Cl]^+ + Cl^- \leftrightarrows \{[L^1H\cdots Cl]\cdots Cl\} \quad (2)$$

It has to be noticed that formation of an outer-spher complex with Cl^- takes place also in the case of the model complex $[Ru^{II}(terpy)_2]^{2+}$, as indicated by a ^{1}H NMR titration experiment on a CD_3CN solution of 4.04×10^{-3} M $[Ru^{II}(terpy)_2](PF_6)_2$. In particular, Figure 5 shows the titration profiles based on the chemical shift of protons 1 and 5 of each coordinated terpy molecule, which undergo a definite downfield shift, indicative of a through-space electrostatic interaction with Cl^-, within the $\{[Ru^{II}(terpy)_2]\cdots Cl\}^+$ outer sphere complex. On nonlinear least-squares treatment of titration data,[14] log K = 1.96 ± 0.01 was calculated for equilibrium 3:

$$[Ru(terpy)_2]^{2+} + Cl^- \leftrightarrows \{[Ru(terpy)_2]\cdots Cl\}^+ \quad (3)$$

On the other hand, on curve fitting the titration profiles reported in Figure 3, which pertain to the outer-sphere interaction of a second Cl^- ion with the $[L^1H\cdots Cl]^+$ complex, log K_2 = 1.7 ± 0.1 was obtained for equilibrium 2. A lower value

dx.doi.org/10.1021/ic400196a | Inorg. Chem. 2013, 52, 5273−5283

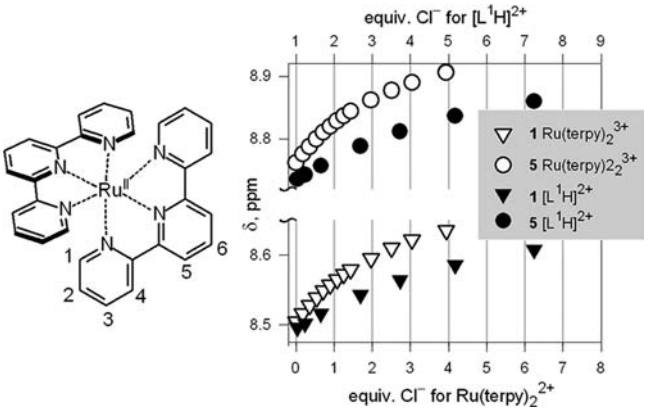

Figure 5. ^{1}H NMR titration of a 3.89 × 10^{-3} M solution of $[Ru(terpy)_2](PF_6)_2$ in CD_3CN with $[Bu_4N]Cl$; profiles based on the chemical shift (δ, ppm) of protons 1 and 5 (open symbols, lower horizontal axis)). Full symbols refer to the chemical shift of protons 1 and 5 of $[L^1H]^{2+}$ observed in the titration in Figure 3, after the addition of 1 equiv of Cl^- (upper horizontal axis). δ values taken from spectra in Figure S7, Supporting Information, and Figure 4.

of K_2 (eq 2) with respect to K (eq 3) is expected on a mere statistical basis: $[L^1H\cdots Cl]^+$ makes available to the electrostatic interaction with Cl^- roughly one-half of the Ru^{II} coordination sphere, due to the presence of the urea···Cl^- substituent on one of the terpy moieties. Moreover, an electrostatic factor can play some role. In fact, the outer-sphere Cl^- ion interacts with a monopositive species, $[L^1H\cdots Cl]^+$, compared with the dication $[Ru(terpy)_2]^{2+}$.

Figure 6 shows the distribution of the species present at the equilibrium over the course (i) of the spectrophotometric titration (concentration of $[L^1H]^{2+}$ = 2.0 × 10^{-5} M, Figure 6a) and (ii) of the ^{1}H NMR titration (concentration of $[L^1H]^{2+}$ = 3.5 × 10^{-3} M, Figure 6b).

In the more diluted solution used in the spectrophotometric titration, the outer-sphere complex $\{[L^1H\cdots Cl]\cdots Cl\}$ does not form in a significant amount and the titration profile based on the absorbance of the MLCT band (at 500 nm) fits quite well the concentration profile of the H-bond complex $[L^1H\cdots Cl]^+$ (see Figure 6a). In the more concentrated solution, both $[L^1H\cdots Cl]^+$ and $\{[L^1H\cdots Cl]\cdots Cl\}$ form over the course of the ^{1}H NMR titration, and titration profiles based on selected protons of the two coordinated terpy moieties overlap satisfactorily on the concentration profiles of the H-bond complex (proton 5′) and of the outer-sphere complex (proton 5, see Figure 6b). Thus, it appears that the two experiments are complementary and help to define accurately the $[L^1H]^{2+}/Cl^-$ equilibrium: the UV−vis titration of the more diluted solution allows the determination of the association constant for the H-bond complex $[L^1H\cdots Cl]^+$, while the ^{1}H NMR titration of the more concentrated solution makes possible the discovery and characterization of the outer-sphere complex $\{[L^1H\cdots Cl]\cdots Cl\}$.

Analogous UV−vis titration experiments were carried out with the tetrabutylammonium salts of Br^-, I^-, NO_2^-, and NO_3^-. In all cases, best fitting of titration data was obtained assuming the formation of a H-bond complex of 1:1 stoichiometry, $[L^1H\cdots X]^+$. The log K values for the corresponding equilibria are shown in Table 1. The trend of

Table 1. The log K Values for the Formation of H-Bond Receptor−Anion Complexes Involving $[L^1H]^{2+}$ and $[L^2H]^{2+}$ in MeCN at 25 °C

	log K, $[L^1H]^{2+}$ + X^- ⇆ $[L^1H\cdots X]^+$	log K, $[L^2H]^{2+}$ + X^- ⇆ $[L^2H\cdots X]^+$	log K,[a] $L^4H]^{2+}$ + X^- ⇆ $[L^4H\cdots X]^+$
Cl^-	5.66 ± 0.01	6.31 ± 0.02	4.55
Br^-	4.84 ± 0.01	5.13 ± 0.01	3.22
I^-	3.98 ± 0.01	4.44 ± 0.01	2.00
NO_2^-	5.51 ± 0.02	5.93 ± 0.01	4.33
NO_3^-	4.38 ± 0.01	4.53 ± 0.01	3.65

[a]Values from ref 5a.

anion affinities is that typically observed for the interaction with H-bond donating receptors, in the absence of relevant steric constraints. For monatomic anions, the affinity decreases along the series Cl^- > Br^- > I^-, which parallels the decrease of the charge density of the anion.[20] In the case of oxoanions, affinity decreases with the decreasing basicity of the anion: NO_2^- > NO_3^-.[21]

The Interaction of $[L^2H]^{2+}$ with Anions in Solution. The spectrophotometric response of receptor $[L^1H]^{2+}$ can be improved by covalently linking to the urea subunit a second powerful chromophore, a 4-nitrophenyl substituent, thus giving $[L^2H]^{2+}$.

Urea derivatives containing 4-nitrophenyl substituents typically show an intense absorption band at ∼350 nm, which results from a charge transfer transition from the urea nitrogen atom to the $-NO_2$ group, across the phenyl ring. The

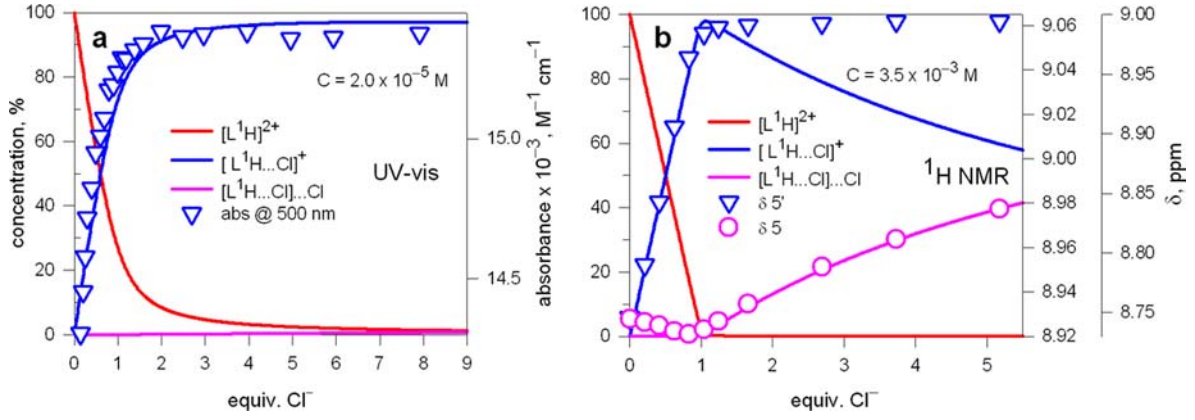

Figure 6. (lines) Distribution of the species present at the equilibrium over the course of the titration with chloride of a solution of $[L^1H]^{2+}$ (a) 2.0 × 10^{-5} M (UV−vis titration) and (b) 3.5 × 10^{-2} M (^{1}H NMR titration,). Symbols: (a) absorbance at 500 nm; (b) chemical shift for protons 5 and 5′.

dx.doi.org/10.1021/ic400196a | Inorg. Chem. 2013, 52, 5273−5283

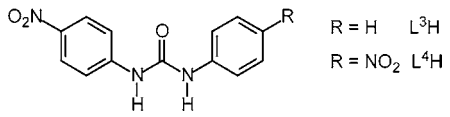

spectrum of 1-(4-nitrophenyl)-3-phenylurea, L^3H, is shown as an example in Figure 7 (blue solid line).

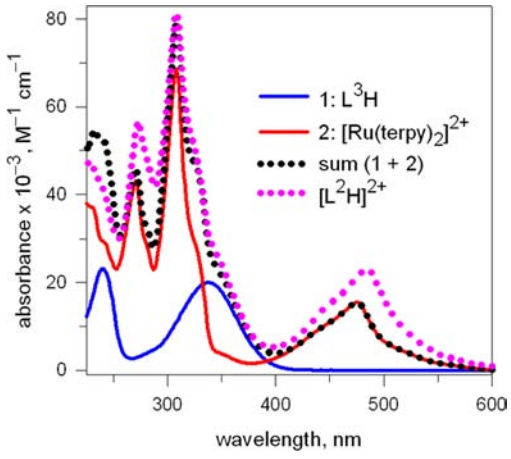

Figure 7. Spectra in MeCN solution of L^3H, $[Ru(terpy)_2](PF_6)_2$, and $[L^2H](PF_6)_2$. Black dotted line results from the sum of spectra of L^3H and $[Ru(terpy)_2](PF_6)_2$.

The spectrum of $[L^2H]^{2+}$ (pink dotted line in Figure 7), which contains both a $Ru(terpy)_2^{2+}$ and a 4-nitrophenyl substituent, is evidently very close to that resulting from the sum of the spectra of L^3H and of $[Ru(bpy)_2]^{2+}$ (black dotted line). In particular, the charge transfer transition associated with the nitrophenyl substituent appears as a shoulder at 350 nm, partially masked by a more intense $\pi-\pi^*$ transition from terpy moieties.

Figure 8a shows the spectra taken over the course of the titration of a MeCN solution of 2.00×10^{-5} M $[L^2H](PF_6)_2$ with a standard solution of $[Bu_4N]Cl$. On chloride addition, a significant bathochromic shift of the shoulder at ~350 nm is observed (see Figure 8b). The corresponding titration profile, shown in Figure 8c, indicates the formation of a 1:1 receptor–anion complex, to which log $K = 6.32 \pm 0.02$ corresponds.

On the other hand, ^1H NMR titration with $[Bu_4N]Cl$ of a CD_3CN solution of 3.47×10^{-3} M $[L^2](PF_6)_2$ disclosed features similar to those observed with $[L^1H]^{2+}$.

In particular, the N_2 proton undergoes downfield shift, which sharply ends on addition of 1 equiv of chloride, as shown in Figure 9a. The N_1 proton shows a broad and poorly defined signal, which does not allow the drawing of a clear titration profile. The interaction of a first Cl^- ion with the urea subunit can be also monitored through the moderate downfield shift of protons 4′ and 5′. Moreover, also in the present case, the formation of an outer-sphere complex $\{[L^2H\cdots Cl]\cdots Cl\}$ is observed, as demostrated by the behavior of protons 1 and 5, which experience a very moderate upfield shift over the 0–1 equiv addition of chloride, then undergo a definite downfield shift on excess addition of the anion (see Figure 9c). Nonlinear least-squares treatment of titration data gave log $K_2 = 1.6 \pm 0.1$ for the equilibrium

$$[L^2H\cdots Cl]^+ + Cl^- \leftrightarrows \{[L^2H\cdots Cl]\cdots Cl\} \quad (4)$$

Spectrophotometric titration experiments on diluted MeCN solutions of $[L^2H]^{2+}$ indicated the formation of 1:1 complexes with Br^-, I^-, NO_2^-, and NO_3^-, whose association constants are reported in Table 1. These values are slightly larger (0.3–0.5 log units) than those observed for $[L^1H]^{2+}$, which may be ascribed to the increased acidity of the urea subunit due to the additional electron-withdrawing effect exerted by the nitrophenyl substituent. Table 1 reports also log K values referring to the anion complex formation of the neutral urea-based receptor L^4H, bearing two nitrophenyl substituents.[5a] These values are 1–2 log units lower than those determined for L^2H, which suggests that the combined electrostatic effect (through-space) and the electron-withdrawing effect (through-bond) exerted by the $Ru(terpy)_2^{2+}$ substituent is more effective than the simple through-bond effect by the neutral nitrophenyl group.

Interaction with Fluoride: Complex Formation and N–H Deprotonation. The fluoride ion plays a unique role in the interaction with urea-based receptors equipped with electron-withdrawing substituents: in a first step, as the anion of the most electronegative element, it establishes strong hydrogen-bonding interactions with the N–H fragments, forming a very stable 1:1 complex. Then, on addition of a second F^-, an N–H proton is abstracted from the receptor, with simultaneous formation of the most stable of H-bond

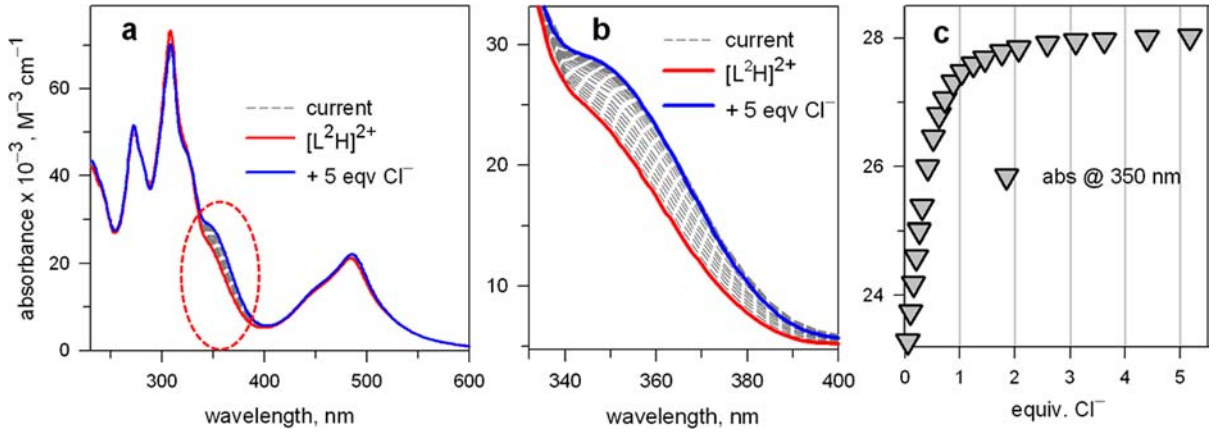

Figure 8. (a) Spectra taken over the course of the titration of a MeCN solution of 2.00×10^{-5} M $[L^2H](PF_6)_2$ with a standard solution of $[Bu_4N]Cl$; (b) close-up of the charge transfer band involving the nitrophenyl moiety; (c) titration profile based on the nitrophenyl band.

dx.doi.org/10.1021/ic400196a | Inorg. Chem. 2013, 52, 5273–5283

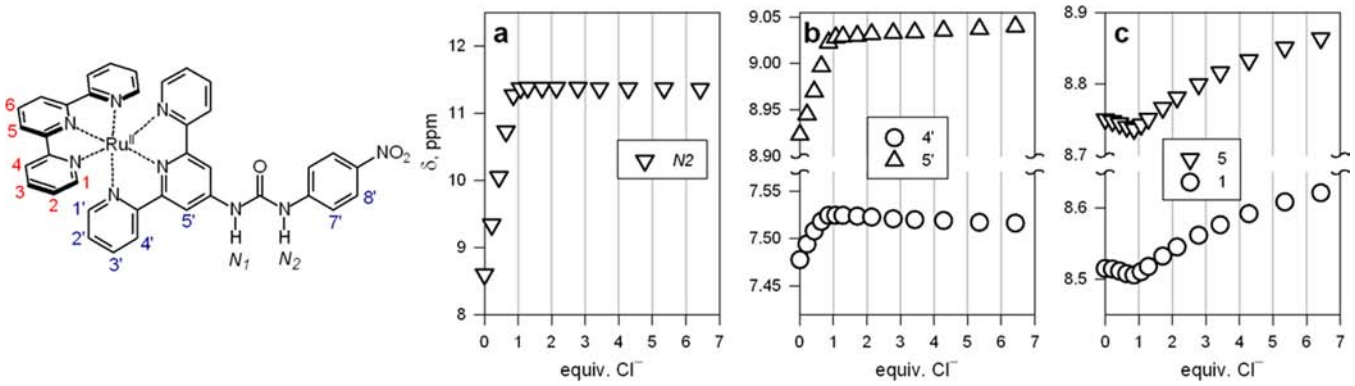

Figure 9. ^{1}H NMR titration profiles, based on the chemical shifts δ, for a CD_3CN solution 3.47×10^{-3} M in $[L^2H](PF_6)_2$ titrated with a standard solution of $[Bu_4N]Cl$. δ values taken from spectra in Figure S9, Supporting Information.

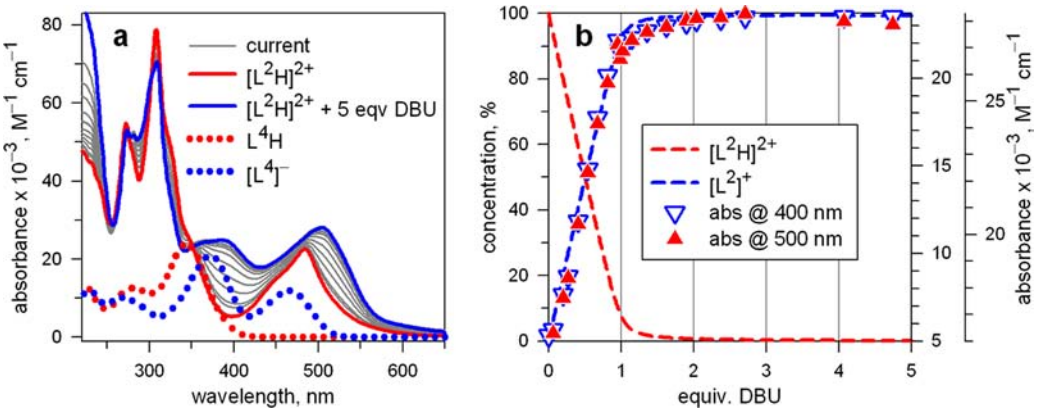

Figure 10. (a) Family of spectra (solid lines) recorded over the course of the titration of a 2.00×10^{-4} M solution of $[L^2H]^{2+}$ in MeCN with a standard solution of DBU; spectra in MeCN of L^4H (red dotted line) and of its deprotonated form $[L^4]^-$ (blue dotted line); (b) concentration profiles (lines) of the species at the equilibrium over the course of the titration; absorbances (symbols) at 400 nm and at 500 nm measured during the titration with DBU.

Scheme 1. The Two Forms of $[L^2]^{+a}$

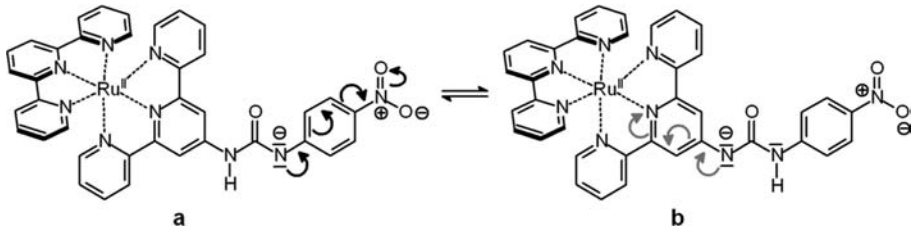

[a]Charge delocalization over the two urea substituents, through a π mechanism, is tentatively illustrated.

complexes, HF_2^-. Such a behavior was first documented for the interaction with the urea derivative L^4H,[5a] for which the two stepwise equilibria were observed:

$$L^4H + F^- \leftrightarrows [L^4H\cdots F]^- \quad (5)$$

$$[L^4H\cdots F]^- + F^- \leftrightarrows [L^4]^- + HF_2^- \quad (6)$$

In particular, the occurrence of the two processes could be characterized through spectrophotometric titrations in MeCN.

Figure 10a shows the spectrum of a MeCN solution of L^4H (red dotted line). Formation of the $[L^4H\cdots F]^-$ H-bond complex induces a bathochromic shift (of ca. 20 nm) of the band at 375 nm. Then, the occurrence of the second step is signaled by the development of a new band at 475 nm, pertinent to the $[L^4]^-$ species (blue dotted line in Figure 10a). Specifically, the bands at 375 and 475 nm originate from charge-transfer transitions from the deprotonated urea fragment to the nitrophenyl subsituent.

The occurrence of similar equilibria is expected for the interaction of fluoride with receptors $[L^1H]^{2+}$ and $[L^2H]^{2+}$, which are more acidic than L^4H. However, in order to characterize the nature and properties of the deprotonated forms $[L^1]^+$ and $[L^2]^+$, preliminary investigations were carried out on the reactions of $[L^1H]^{2+}$ and $[L^2H]^{2+}$ with 1,8-diazabicyclo[5.4.0]undec-7-ene (DBU). DBU is a very strong base, with pK_a = 24.13, in MeCN at 25 °C.[22] In particular, a 2.00×10^{-4} M solution of $[L^2H]^{2+}$ in MeCN was titrated with a standard solution of DBU. The family of spectra recorded over the course of the titration is shown in Figure 10a. Addition of the strong base induces significant spectral changes, with the

dx.doi.org/10.1021/ic400196a | Inorg. Chem. 2013, 52, 5273−5283

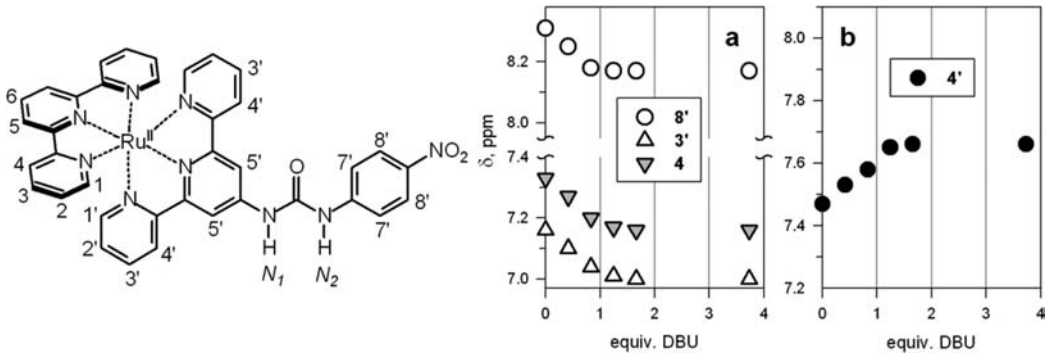

Figure 11. ^{1}H NMR titration profiles, based on the chemical shifts, δ, for a CD_3CN solution of 3.21×10^{-3} M $[L^2H](PF_6)_2$ titrated with a standard solution of DBU. Values taken from spectra in Figure S11, Supporting Information.

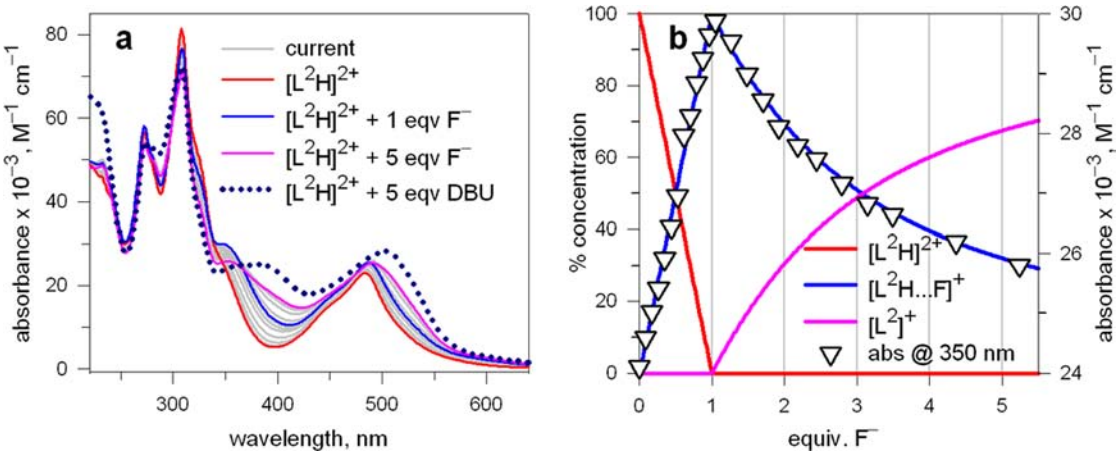

Figure 12. (a) Family of spectra (solid lines) taken over the course of the titration with fluoride of an MeCN solution of 2.00×10^{-4} M $[L^2H](PF_6)_2$; spectra of an MeCN solution of L^4H (red dotted line) and of $[L^4]^-$ (pink dotted line). (b) Concentration of the species present at the equilibrium over the course of the titration (lines, left vertical axis), calculated assuming $\log K_1 = 9.0$ and $\log K_2 = 3.5$; titration profile (symbols, right vertical axis) at 350 nm.

development of new intense bands at 400 and 500 nm. It is suggested that the new bands pertain to the deprotonated species $[L^4]^+$, which forms in the neutralization equilibrium 7:

$$[L^2H]^{2+} + DBU \leftrightarrows [L^2]^+ + DBUH^+ \quad (7)$$

Notice that $[L^2]^+$ may exist as an equilibrium mixture of two forms, a and b, in which deprotonation has occurred at either N−H fragment, as illustrated in Scheme 1.

In particular, the new bands at 400 and 500 nm seem to pertain to form a, resulting from charge-transfer transitions from the deprotonated N−H fragment to the adjacent nitrophenyl substituent. On the other hand, the negative charge originated by the deprotonation of the N−H fragment close to the $Ru(terpy)_2^{2+}$ subunit, in form b, may delocalize to the nitrogen atoms of the terpy substituent and, from there, through the metal center, to the coordinated plain terpy molecule. While this mechanism should alter MO levels of the $Ru^{II}(terpy)_2^{2+}$ subunit, thus modifying $\pi-\pi^*$ and MLCT transitions, corresponding spectral changes cannot be unambiguously assigned and characterized. In any case, titration profiles based on absorbances at 400 and 500 nm, reported in Figure 10b, clearly indicated the 1:1 stoichiometry of equilibrium 7. Through nonlinear least-squares treatment of spectrophotometric data,[19] $\log K = 5.87 \pm 0.01$ was determined for the neutralization equilibrium 7. Lines in Figure 10b represent the concentrations of $[L^2H]^{2+}$ and $[L^2]^+$ over the course of the titration, as calculated from the log K value. Notice that absorbances at 400 and 500 nm (symbols in Figure 10b) fit well the concentration profile of $[L^2]^+$.

However, ^{1}H NMR titration allowed us to define more clearly how deprotonation of $[L^2H]^{2+}$ takes place, directly indicating the coexistence of the two species a and b. In particular, Figure 11 shows the significant chemical shifts, δ, of some selected protons.

On titration, a defined upfield shift is observed for proton 8′, which indicates that in the form deprotonated at N_2, formula a in Scheme 1, electrons are delocalized on the aromatic ring of the nitrophenyl substituent via a through-bond mechanism. On the other hand, the upfield shift experienced by proton 3′ suggests that a similar mechanism operates in the $[L^2]^+$ form deprotonated at N_1 (formula b in Scheme 1). Very significantly, a chemical shift of the same extent is observed also for proton 4, belonging to the coordinated plain terpy molecule, which implies that transfer of some electron charge takes place through the Ru^{II} center. Moreover, proton 4′ undergoes a significant downfield shift (Figure 11b), pointing toward the predominance of a through-space effect. This may be due to the electrostatic interaction of proton 4′ with the carbonyl oxygen atom, which may assume a partial negative charge on N−H deprotonation (through a delocalization mechanism not illustrated in Scheme 1).

The spectroscopic features of the deprotonated form $[L^2]^+$ being clear, titrations of $[L^2H]^{2+}$ with fluoride were carried out.

dx.doi.org/10.1021/ic400196a | Inorg. Chem. 2013, 52, 5273−5283

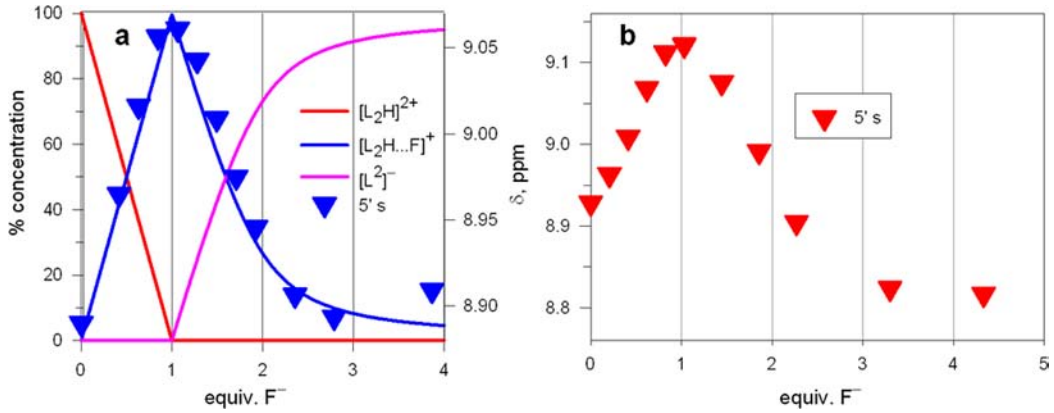

Figure 13. ^{1}H NMR titration of CD_3CN solutions of (a) 3.21×10^{-3} M $[L^2H](PF_6)_2$ and (b) 3.36×10^{-3} M $[L^1H](PF_6)_2$ with a standard solution of $[Bu_4N]F{\cdot}3H_2O$. Titration profiles based on the chemical shift, δ, of proton 5′. Values in panel b taken from spectra in Figure S12, Supporting Information; values in panel a taken from spectra in Figure S13, Supporting Information. Panel a also displays the concentration of the species present at equilibrium over the course of the titration (solid lines), calculated for log K (eq 8) = 9.0 and log K (eq 9) = 3.5.

Figure 12a (solid lines) shows the family of spectra taken over the course of the spectrophotometric titration with fluoride of an MeCN solution of 2.00×10^{-4} M $[L^2H](PF_6)_2$. The dotted line represents the spectrum of a 2.00×10^{-4} M $[L^2H](PF_6)_2$ solution plus 5 equiv of DBU, thus containing 100% of the deprotonated species $[L^2]^+$, which has been reported for comparative purposes.

On titration with F^-, a general increase of the absorption is observed in the 350−550 nm interval, which can be ascribed to the development of the low-energy bands pertinent to the deprotonated nitrophenyl−urea moiety. However, $\pi-\pi^*$ and MLCT based absorptions overlap with the absorption due to the nitrophenyl chromophore, making a quantitative interpretation of titration data difficult and preventing an accurate description of the system. The most significant spectral changes are observed at 330−350 nm, where a bathochromic shift of the shoulder assigned to the urea-to-nitrophenyl transition takes place on addition of the first equivalent of F^- to form a defined band. Then, on addition of more F^-, the intensity of this band distinctly decreases. The change of the absorption intensity at 350 nm (symbols in Figure 12b) is especially indicative: a steep increase of the absorbance is observed on addition of the first equivalent of F^-, which is followed by a more gentle decrease on excess anion addition. It is suggested that the absorbance at 350 nm pertains to the H-bond complex, $[L^2H{\cdots}F]^+$, which reaches its highest concentration (presumably 100%) with the addition of 1 equiv of fluoride. Then, deprotonation of one N−H fragment takes place, with which a decrease of the band at 350 nm and of the concentration of the $[L^2H{\cdots}F]^+$ complex, are associated. The sharp discontinuity of the ascending and descending portions of the profile implies a very high value for the association constant of the H-bond complex. On the other hand, a particularly high value is expected, if one considers (i) that the corresponding log K value for L^4H is 7.6 and (ii) that $[L^2H]^{2+}$ forms with halide ions complexes 1−2 orders of magnitude more stable than L^4H. Figure 12b reports also the variation of the concentration (%) of the species at the equilibrium during the titration, calculated tentatively assuming log K_1 = 9.0 (formation of the H-bond complex, eq 8) and log K_2 = 3.5 (deprotonation equilibrium, eq 9). This couple of values ensures the best superimposition of absorbance at 350 nm on the concentration profile of $[L^2H{\cdots}F]^+$, thus confirming the occurrence of the stepwise equilibria 8 and 9:

$$[L^2H]^{2+} + F^- \leftrightarrows [L^2H{\cdots}F]^+ \quad (8)$$

$$[L^2H{\cdots}F]^+ + F^- \leftrightarrows [L^2]^+ + HF_2^- \quad (9)$$

More detailed pieces of information on the nature of these species could be obtained from the ^{1}H NMR titration with fluoride of a solution of 3.21×10^{-3} M $[L^2H](PF_6)_2$ in CD_3CN (Figure S13 in Supporting Information). The most significant change of chemical shift is that pertaining to proton 5′ and is shown in Figure 13a.

On addition of the first equivalent of F^-, the signal undergoes a well-defined downfield shift, a behavior consistent with the formation of the H-bond complex, as described by eq 9. In particular, the through-space effect due to the electrostatic interaction with the H-bonded fluoride ion (and on the carbonyl oxygen atom, on which partally negative electrical charge has been transferred) predominates over the through-bond effect. On addition of excess of F^-, the signal undergoes a neat upfield shift, a behavior in agreement with the occurrence of eq 9. In fact, the negative charge originated from the deprotonation of the N−H fragment substantially delocalizes, through a conjugative mechanism, onto the central heterocyclic ring of the terpy subunit linked to urea, inducing a pronounced upfield effect. Noticeably, the profile of the chemical shift fits quite reasonably the calculated concentration profile of the $[L^2H{\cdots}F]^+$ complex (see symbols in Figure 13a), confirming the reliability of the model.

Titration with DBU showed that $[L^1H]^{2+}$ is a monoprotic acid (log K of the neutralization equilibrium = 5.15 ± 0.01), slightly weaker than $[L^2H]^{2+}$, which contains the nitrophenyl substituent. The limiting spectrum obtained in the presence of 5 equiv of DBU, thus pertaining to $[L^1]^+$, is shown in Figure 14, as a dotted line.

The spectrophotometric titration of $[L^1H](PF_6])_2$ in MeCN with fluoride induced spectral changes less significant than those observed with the $[L^2H]^{2+}$ derivative yet more pronounced than those observed in the titration of $[L^1H]^{2+}$ with chloride and other inorganic anions. The family of spectra obtained on titration of a solution of 2.07×10^{-4} M $[L^1H](PF_6])_2$ with F^- is shown in Figure 14 (solid lines). Occurrence of deprotonation is suggested by the increase of absorbance at ca. 350 and 530 nm. However, spectral changes are not definite enough to allow a quantitative asssessment of the equilibria that take place. On the other hand, the

dx.doi.org/10.1021/ic400196a | Inorg. Chem. 2013, 52, 5273−5283

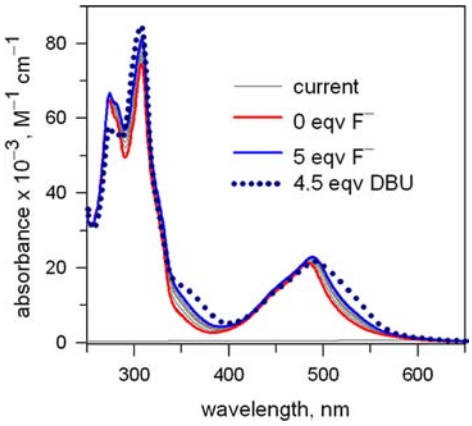

Figure 14. Family of spectra (solid lines) taken over the course of the titration with fluoride of an MeCN solution of 2.07×10^{-4} M $[L^1H](PF_6)_2$; spectrum of an MeCN solution of $[L^1H]^{2+}$ in the presence of an excess of DBU (dotted line), thus containing 100% of the deprotonated form $[L^1]^+$.

occurrence of a two-step interaction of $[L^1H]^{2+}$ with fluoride, described by equilibria of type 8 and 9, is clearly indicated by the ^{1}H NMR titration, in particular by the profile of the chemical shift experienced by proton 5′, reported in Figure 13b. The profile is analogous to that observed for the $[L^2H]^{2+}$, showing an ascendent (up to 1 equiv of F^-), then a descendent arm, with some significant differences: (i) the extent of the upfield shift observed on addition of excess fluoride is distinctly greater for $[L^1H]^{2+}$ than for $[L^2H]^{2+}$; this may be because in the absence of the electron-withdrawing nitrophenyl substituent, deprotonation takes place mainly at the N−H fragment close to the $Ru(terpy)_2^{2+}$ subunit, which induces a more pronounced delocalization of negative charge on the heterocyclic rings of the covalently linked terpy; (ii) the chemical shift $\delta(5')$ in $[L^1H]^{2+}$, after the addition of 1 equiv of F^-, decreases less steeply than for $[L^2H]^{2+}$, a behavior ascribed to a less pronounced formation of the deprotonated species in the case of the less acidic receptor $[L^1H]^{2+}$ compared with $[L^2H]^{2+}$.

Luminescence and Redox Behavior of $[L^1H]^{2+}$. The $Ru(terpy)_2^{2+}$ complex is not luminescent at room temperature because the sterically constrained terpy molecule does not exert an especially strong ligand field (as bpy does).[23] As a consequence, the metal-centered excited state, ^{3}MC, is not destabilized enough and a thermally activated transition from the ^{3}MLCT excited state to ^{3}MC can take place, with subsequent nonradiative decay to the ground state. On temperature decrease, the ^{3}LMCT → ^{3}MC thermal transition is made less efficient and luminescence of $Ru(terpy)_2^{2+}$ is revived in a matrix at 77 K. On the other hand, insertion at position 6 of the terpy ligand of an electron-withdrawing/electron-donor substituent may induce an increase of the lifetime of the ^{3}MLCT excited state and an increase of the emission intensity.[14] Apparently, the urea substituent in $[L^1H]^{2+}$ and $[L^2H]^{2+}$ does not behave as a strong electron-withdrawing group, because the two Ru^{II} complexes do not show luminescence in an MeCN solution at room temperature. However, both $[L^1H]^{2+}$ and $[L^2H]^{2+}$ display luminescence in a frozen butyronitrile solution at 77 K. The emission spectrum of $[L^1H](PF_6)_2$ (λ_{exc} = 490 nm, see Figure S14, Supporting Information) shows that the ^{3}MLCT emission band (λ_{max} = 614 nm) is bathochromically shifted with respect to $Ru(terpy)_2^{2+}$ (λ_{max} = 598 nm), a feature typically imparted by substitution at position 6 by electron-withdrawing/electron-donor substituents.[14] In any case, the absence of a luminescent emission at room temperature prevents or makes rather difficult the accomplishment of titration experiments with anions.

The $Ru(terpy)_2^{2+}$ complex undergoes electrochemically reversible metal-centered one-electron oxidation at a rather anodic potential. Thus, the electrode potential associated with the $Ru^{III}(terpy)_2^{3+}/Ru^{II}(terpy)_2^{2+}$ couple of the $[L^1H]^{2+}$ receptor, measured in voltammetric titration experiments, could monitor the interaction with anions, provided that they are resistant to the oxidation. Cyclic voltammetry (CV) and differential pulse voltammetry (DPV) studies at a platinum working electrode on an MeCN solution of 1.00×10^{-4} M $[L^1H]^{2+}$ and 0.05 M background electrolyte ($[Bu_4N]PF_6$) showed the occurrence of a very moderate cathodic shift of $E_{1/2}$ on addition of $[Bu_4N]NO_3$ (~20 mV in the presence of 20 equiv of anion, see Figure S15, Supporting Information). Indeed, one would expect that a +2 to +3 increase of the electrical charge of the proximate metal center induces a substantial enhancement of the association constant, to which a significant decrease of $E_{1/2}$ should correspond. However, in the present experiments, the anion of the background electrolyte, PF_6^-, present in a 500-fold excess, can compete for the interaction at the urea subunit, thus decreasing the affinity for NO_3^- of both reduced and oxidized forms of the receptor. On titration with the other investigated oxidation-resistant anion, fluoride, anion additions induced a broadening of the DPV peak and a decrease of the current intensity. At the same time, the formation of a dark powder on the working electrode was observed, which indicated the formation of an insoluble oxidation product and prevented any reliable investigation.

CONCLUSION

The $Ru(terpy)_2^{2+}$ substituent undergoes small yet significant modifications of its $\pi-\pi^*$ and MLCT bands on anion interaction with a covalently linked urea moiety, a circumstance that allows the safe determination of especially high anion−receptor association constants in MeCN. However, $Ru(terpy)_2^{2+}$ cannot compete as an optical reporter with classical organic chromophores like the nitrophenyl substituent, whose charge transfer transitions are directly and profoundly modified, in energy and intensity, by the anion−urea interaction. On the other hand, $Ru(terpy)_2^{2+}$ enhances the affinity toward anions of the linked urea subunit to a larger extent than the powerful electron-withdrawing group nitrophenyl. The $Ru(terpy)_2^{2+}$ advantage seems to result from (i) an electrostatic (through-space) effect and (ii) a covalent (through-bond) effect. As far as point i is concerned, it is suggested that the urea bound anion (through a H-bond interaction) experiences an additional Coulombic attraction by the nearby positively charged metal center. Noticeably, the $Ru(terpy)_2^{2+}$ substituent itself is capable of interacting with a second chloride ion via an outer-sphere mechanism, through a purely electrostatic interaction. Concerning point ii, ^{1}H NMR experiments have demonstrated that the electronic charge brought by the H-bonded anion (e.g., Cl^-) is transferred not only to the nearby terpy fragment but also to the ancillary terpy ligand, according to a transmission mechanism that must involve the Ru^{II} center. The positive charge and the electron-withdrawing properties of $Ru(terpy)_2^{2+}$ favor the deprotonation of one N−H fragment in the presence of excess fluoride, a process that has been independently characterized by both spectrophotometric and ^{1}H NMR titration experiments.

dx.doi.org/10.1021/ic400196a | Inorg. Chem. 2013, 52, 5273−5283

There exists a vast body of literature on anion recognition and sensing based on the direct interaction of the analyte with a coordinatively unsaturated metal center.[24,25] It has been shown here that metals, even when coordinatively saturated, can play a valuable role in anion recognition, by enhancing the H-bond donor tendencies of a covalently linked N−H containing receptor. Such an enhancing effect can be modulated by varying the nature of the metal and of its ligand. Studies along this line are underway in our laboratory.

EXPERIMENTAL SECTION

General methods and procedures, synthesis, and characterization of receptors $[L^1H]^{2+}$ and $[L^2H]^{2+}$ and crystal structure determination studies on $[L^1H](PF_6)_2$ are described in detail in the Supporting Information, in which families of spectra from titration experiments (both UV−vis and ^{1}H NMR) are also shown. CCDC 916540 contains the supplementary crystallographic data for this paper. These data can be obtained free of charge via www.ccdc.cam.ac.uk/conts/retrieving.html (or from the Cambridge Crystallographic Data Centre, 12 Union Road, Cambridge CB21EZ, UK; fax (+44) 1223-336-033 or e-mail deposit@ccdc.cam.ac.uk).

ASSOCIATED CONTENT

Supporting Information

X-ray crystallographic files in CIF format for the $[L^1H](PF_6)_2 \cdot 1.75H_2O$ salt and details of the synthesis and characterization of $[L^1H](PF_6)_2$ and $[L^2H](PF_6)_2$ and of spectrophotometric and ^{1}H NMR titration experiments. This material is available free of charge via the Internet at http://pubs.acs.org.

AUTHOR INFORMATION

Corresponding Author

*E-mail: luigi.fabbrizzi@unipv.it.

Notes

The authors declare no competing financial interest.

ACKNOWLEDGMENTS

The financial support of the Italian Ministry of University and Research (PRIN−Infochem) is gratefully acknowledged.

REFERENCES

(1) (a) *Anion Coordination Chemistry*; Bowman-James, K., Bianchi, A., García-España, E., Eds; Wiley-VCH: Weinheim, Germany, 2011. (b) Santos-Figueroa, L. E.; Moragues, M. E.; Climent, E.; Agostini, A.; Martínez-Máñez, R.; Sancenón, F. *Chem. Soc. Rev.* **2013**, *42*, 3489−3613. (c) Wenzel, M.; Hiscock, J. R.; Gale, P. A. *Chem. Soc. Rev.* **2012**, *41*, 480−520.

(2) (a) Li, A.-F.; Wang, J.-H.; Wang, F.; Jiang, Y.-B. *Chem. Soc. Rev.* **2010**, *39*, 3729−3745. (b) Amendola, V.; Fabbrizzi, L.; Mosca, L. *Chem. Soc. Rev.* **2010**, *39*, 3889−3915. (c) Hossain, M. A.; Begum, R. A.; Day, V. W.; Bowman-James, K. *Supramol. Chem.: Mol. Nanomater.* **2012**, *3*, 1153−1178.

(3) Smith, P. J.; Reddington, M. V.; Wilcox, C. S. *Tetrahedron Lett.* **1992**, *33*, 6085−6088.

(4) Fan, E.; van Arman, S. A.; Kincaid, S.; Hamilton, A. D. *J. Am. Chem. Soc.* **1993**, *115*, 369−370.

(5) (a) Boiocchi, M.; Del Boca, L.; Esteban-Gómez, D.; Fabbrizzi, L.; Licchelli, M.; Monzani, E. *J. Am. Chem. Soc.* **2004**, *126*, 16507−16514. (b) Boiocchi, M.; Del Boca, L.; Esteban-Gómez, D.; Fabbrizzi, L.; Licchelli, M.; Monzani, E. *Chem.—Eur. J.* **2005**, *11*, 3097−3104. (c) Esteban-Gómez, D.; Fabbrizzi, L.; Licchelli, M. *J. Org. Chem.* **2005**, *70*, 5717−5720. (d) Esteban-Gómez, D.; Fabbrizzi, L.; Licchelli, M.; Monzani, E. *Org. Biomol. Chem.* **2005**, *3*, 1495−1500.

(6) Amendola, V.; Esteban-Gómez, D.; Fabbrizzi, L.; Licchelli, M. *Acc. Chem. Res.* **2006**, *39*, 343−353.

(7) Szemes, F.; Hesek, D.; Chen, Z.; Dent, S. W.; Drew, M. G. B.; Goulden, A. J.; Graydon, A. R.; Grieve, A.; Mortimer, R. J.; Wear, T.; Weightman, J. S.; Beer, P. D. *Inorg. Chem.* **1996**, *35*, 5868−5879.

(8) Beer, P. D. *Acc. Chem. Res.* **1998**, *31*, 71−80.

(9) Beer, P. D.; Dent, S. W.; Wear, T. *J. Chem. Soc., Dalton Trans.* **1996**, 2341−2346.

(10) Beer, P. D.; Cadman, J. *New J. Chem.* **1999**, *23*, 347−350.

(11) Beer, P. D.; Timoshenko, V.; Maestri, M.; Passaniti, P.; Balzani, V. *Chem. Commun.* **1999**, 1755−1756.

(12) Constable, E. C. *Chem. Soc. Rev.* **2007**, *36*, 246−253.

(13) Sauvage, J.-P.; Collin, J.-P.; Chambron, J.-C.; Guillerez, S.; Coudret, C.; Balzani, V.; Barigelletti, F.; De Cola, L.; Flamigni, L. *Chem. Rev.* **1994**, *94*, 993−1019.

(14) (a) Constable, E. C.; Cargill Thompson, A. M. W.; Armaroli, N.; Balzani, V.; Maestri, M. *Polyhedron* **1992**, *11*, 2707−2709. (b) Maestri, M.; Armaroli, N.; Balzani, V.; Constable, E. C.; Cargill Thompson, A. M. W. *Inorg. Chem.* **1995**, *34*, 2759−2767. (c) Wang, J.; Fang, Y. Q.; Hanan, G. S.; Loiseau, F.; Campagna, S. *Inorg. Chem.* **2005**, *44*, 5−7.

(15) Padilla-Tosta, M. E.; Lloris, J. M.; Martínez-Máñez, R.; Pardo, T.; Soto, J.; Benito, A.; Marcos, M. D. *Inorg. Chem. Commun.* **2000**, *3*, 45−48.

(16) Padilla-Tosta, M. E.; Lloris, J. M.; Martínez-Máñez, R.; Pardo, T.; Sancenón, F.; Soto, J.; Marcos, M. D. *Eur. J. Inorg. Chem.* **2001**, 1221−1226.

(17) (a) Bhaumik, C.; Saha, D.; Das, S.; Baitalik, S. *Inorg. Chem.* **2011**, *50*, 12586−12600. (b) Bhaumik, C.; Maity, D.; Das, S.; Baitalik, S. *Polyhedron* **2013**, *52*, 890−899.

(18) Allen, F. H. *Acta Crystallogr.* **2002**, *B58*, 380−388.

(19) Using the Hyperquad package: Gans, P.; Sabatini, A.; Vacca, A. *Talanta* **1996**, *43*, 1739−1753. http://www.hyperquad.co.uk/index.htm; accessed 24 January, 2013.

(20) Amendola, V.; Bergamaschi, G.; Boiocchi, M.; Fabbrizzi, L.; Milani, M. *Chem.—Eur. J.* **2010**, *16*, 4368−4380.

(21) Baggi, G.; Boiocchi, M.; Fabbrizzi, L.; Mosca, L. *Chem.—Eur. J.* **2011**, *17*, 9423−9439.

(22) Kaljurand, I.; Rodima, T.; Leito, I.; Koppel, I. A.; Schwesinger, R. *J. Org. Chem.* **2000**, *65*, 6202−6208.

(23) Balzani, V.; Scandola, F. *Supramolecular Photochemistry*; Ellis Horwood: New York, 1991.

(24) O'Neil, E. J.; Smith, B. D. *Coord. Chem. Rev.* **2006**, *250*, 3068−3080.

(25) Fabbrizzi, L.; Poggi, A. *Chem. Soc. Rev.* **2013**, *42*, 1681−1699.